Distributed Control of Triangular Formations with Angle-Only Constraints

Meysam Basiri, Adrian N. Bishop and Patric Jensfelt

***Abstract*—This paper considers the coupled formation control of three mobile agents moving in the plane. Each agent has only local inter-agent bearing knowledge and is required to maintain a specified angular separation relative to both neighbor agents. Assuming the desired angular separation of each agent relative to the group is feasible, then a triangle is generated. The control law is distributed and accordingly each agent can determine their own control law using only the locally measured bearings. A convergence result is established in this paper which guarantees *global asymptotic convergence* of the formation to the desired formation shape.**

I. Introduction

This paper presents a distributed control system for triangular formation control based only on local bearing measurements and relative angular constraints. The formations considered are characterized entirely by the interior angles subtended at each agent by two neighbor agents. The angle-based formation control problem introduced in this paper is a novel contribution in the field of multi-agent dynamical systems and the control law proposed is provably globally asymptotically stabilizing.

Distributed control of multi-agent formations has been explored extensively in different settings. For example, consensus and flocking algorithms lead to formation-like steady-state structures of multi-agent systems [1]–[8]. Similarly, so-called aggregation and swarm control, which typically involves potential functions [9], is also common in the robotics and control literature [10]–[14]. A number of formation control applications have been considered [15]–[20] which typically involve formations of uninhabited aerial or underwater vehicles or formations of satellites etc. The problem considered in this paper follows closely the ideology put forth in [11], [21]–[24]. Specifically we are concerned with the formation, and subsequent maintenance, of specific inter-agent geometric relationships using distributed algorithms. The majority of existing algorithms consider only inter-agent distance measures. We differ from this in a novel way, by considering only inter-agent bearing measures taken in local coordinates, i.e. agents do not share a common heading. Our bearing-only formation control problem is motivated by the problem of optimal sensor arrangement for localization [1], [2] where the relative configurations are typically given in terms of the angular geometry.

The authors are with the Centre for Autonomous Systems (CAS) at the Royal Institute of Technology (KTH), Stockholm Sweden. This work was supported by the Swedish Foundation for Strategic Research (SSF) through CAS and also via the EU FP7 project “CogX”.

There are two fundamental problems which need addressing. Firstly, the number and characteristics of the particular constraints required has to be established. Obviously, defining a complete distance constraint graph between a group of agents will suffice in defining a unique formation. However, defining a certain (well-chosen) subset of these distance constraints can often (generically) define a unique formation, e.g. see [21], [25]–[27]. Directed constraints can also be considered, where some agents are tasked at maintaining a given distance from another agent while the converse is not true, e.g. see [26], [27]. Relative angular constraints can also be considered [28]. Establishing the constraint leads to the second problem of formation control, i.e. the design of control laws. The control laws can either be distributed or centralized. Often, distributed control lends itself naturally to the multi-agent formation control problem and it is this form of control which is considered in this paper. A distributed law for formation control is implemented by individual agents in the formation. Each agent attempts to achieve (and maintain) the desired relevant constraints placed on it’s own position but does not consider the constraints of any other agents (when planning it’s own motion control).

The contribution of this paper is the development of a distributed law for angular constrained formation control of a multi-agent system taking only relative bearing measurements. A large literature exists on bearing-only state estimation and localization [29]–[31] making the angle-based formation control problem particularly appealing. However, despite this fact, angle-based formation control is not commonly addressed in the literature; see [32], [33]. Instead, a large literature in both robotics and control focuses on distance-based formation control and potential-function-based control laws. In this paper, we introduce an angular constrained formation control problem for a group of agents tasked at maintaining a specified triangular formation. The control law introduced in this paper is globally asymptotically stabilizing given any initial agent configuration (assuming no agents are collocated initially). No similar results on provably stable angle-only formation control exist in the literature.

The paper is organized as follows. In Section II, the triangular formation control problem is introduced along with the distributed control law proposed in this paper. Subsequently, the multi-agent system evolution is examined and global stability of the desired formation shape is proved. In Section III a number of illustrative examples are given. Some discussion points are covered in Section IV and a conclusion is given in Section V.

II. Bearing-Only Triangular Formation Control

Consider a group of $n = 3$ agents in $\mathbb{R}^2$ which *interact* via an undirected topology $\mathcal{G} = \{\mathcal{V}, \mathcal{E}\}$ with $\mathcal{V} = \{1, 2, 3\}$ and $\mathcal{E} = \mathcal{V} \times \mathcal{V}$. The position of each agent is

$$\mathbf{p}_i = [x_i \ y_i]^{\mathrm{T}} \in \mathbb{R}^2 \tag{1}$$

where x_i and y_i denote agent i's position in the x and y directions respectively. The neighbor set $\mathcal{N}_i \subset \mathcal{V}$ denotes the set of agents connected to agent i by a single (undirected) edge. In this case $\mathcal{N}_i = \{(i+1), (i-1)\}$ (modulo n).

Importantly, note that agents do *not* share a common heading, i.e. they are not equipped with a compass of any kind. Agent i measures only the bearing $\phi_{ij} \in [-\pi, \pi)$, $\forall j \in \mathcal{N}_i$ positive (negative) counter-clockwise (clockwise) from their local x_i-direction to agent j. Let α_i denote the angle subtended at agent i by the two agents in $\mathcal{N}_i$. Then, the formation shape (not scale) is completely characterized by α_i, $\forall i \in \mathcal{V}$. Introduce the following angle

$$\vartheta_i = |\phi_{i(i+1)} - \phi_{i(i-1)}| \in [0, 2\pi) \tag{2}$$

which is the angle subtended at agent i by agents $i+1$ and $i-1$ which is measured positive from the $\min(\phi_{i(i+1)}, \phi_{i(i-1)})$ to $\max(\phi_{i(i+1)}, \phi_{i(i-1)})$ in agent i's local coordinate frame. Then, mathematically, the interior α_i can be given by

$$\alpha_i = \begin{cases} \vartheta_i & \text{if } \vartheta_i \leq \pi \\ 2\pi - \vartheta_i & \text{otherwise} \end{cases} \tag{3}$$

with $\alpha_i \in [0, \pi]$. Note the difference between $\alpha_i = 0$ and $\alpha_i = \pi$ implies agent i can ascertain whether or not it is in between agents $i+1$ and $i-1$ with all three collinear. Tacitly, it can be assumed that α_i is measured by agent i. The inter-agent range has not been considered and plays no part in the measurement of α_i or the control law to be derived.

Define the desired steady-state angles $\alpha_i^* \in [0, \pi]$, $\forall i \in \mathcal{V}$. The α_i^* then completely characterize the shape (not scale) of the *desired* triangle formation. The following standing assumptions are adopted to hold through Sections II and III.

Assumption 1. *The desired (i.e. control objective) interior angular separations α_i^*, obey $\alpha_1^* + \alpha_2^* + \alpha_3^* = \pi$. The case where $\alpha_i^* = 0$, $\alpha_j^* \neq 0$ and $\alpha_k^* = \pi - \alpha_j^*$ is excluded.*

Assumption 2. *The initial agent positions $\mathbf{p}_i(0)$ are non-coincident, i.e. $\mathbf{p}_i(0) \neq \mathbf{p}_j(0)$, $\forall i \neq j$.*

Assumption 1 ensures the desired steady-state triangle is well-defined and the set of control objectives are simultaneously feasible. The case where $\alpha_i^* = 0$, $\alpha_j^* \neq 0$ and $\alpha_k^* = \pi - \alpha_j^*$ would place agent i infinitely far from the other two agents and this case will be discussed separately later. The considered problem is now summarized.

Problem (Angle-Only Triangle Control)**.** *Design a distributed control law for agent i that steers the measured angle α_i to α_i^* given any initial triangle formation. Technically, as time $t \to \infty$ then we want $\alpha_i \to \alpha_i^*$ exponentially fast given any initial configuration. Moreover, we want α_i to be well-defined for the entire motion of the formation, i.e. no two agent positions should coincide during the formation motion.*

This problem is novel since the controller uses only bearing measurements taken by individual agents in local coordinates and we are given only inter-agent angle constraints. Agents do not share information and agent i does not consider the constraints of any other agent when executing its own control law.

A. The Proposed Control Law

The motion of agent i is governed by

$$\dot{\mathbf{p}}_i = v_i \begin{bmatrix} \cos\beta_i \\ \sin\beta_i \end{bmatrix} \tag{4}$$

where both v_i and β_i are control inputs to be determined. The heading β_i is defined positive (negative) counter-clockwise (clockwise) from agent i's local x_i-direction. The control law which determines v_i and β_i is truly distributed and determined solely by α_i^* and the measured angle α_i subtended at agent i by two agents $j \in \mathcal{N}_i$. The speed control input of agent i is defined as follows,

$$v_i = (\alpha_i^* - \alpha_i)k \tag{5}$$

where $k > 0$ is a constant (which in this paper is taken to be $k = 1$). The heading of agent i is defined along the bisection of $\alpha_i \in [0, \pi]$ and toward the interior of α_i so that

$$\beta_i = \begin{cases} \frac{\alpha_i}{2} + \min(\phi_{i(i+1)}, \phi_{i(i-1)}), & \text{if } \vartheta_i \leq \pi \\ \frac{\alpha_i}{2} + \max(\phi_{i(i+1)}, \phi_{i(i-1)}), & \text{if } \vartheta_i > \pi \end{cases} \tag{6}$$

where ϑ_i is given by (2). Actually, it is easier to visualize the heading of agent i then to mathematically define it. Visually, the heading of agent i is simply toward the interior of α_i and specifically along the bisection of α_i. Of course, the speed of agent i might be negative. By definition, if $\alpha_i = \pi$ then the bisection is well defined by $\frac{\alpha_i}{2} + \min(\phi_{i(i+1)}, \phi_{i(i-1)})$. If $\alpha_i = 0$ then the bisection is also well defined.

The control laws (5) and (6) imply that if $\alpha_i^* > \alpha_i$, so that the angular separation subtended at agent i is too small, then v_i is positive and the agent moves toward the interior of and along the bisection of α_i. Clearly, the description of agent i's movement is coupled to the movements of agents $(i+1)$ and $(i-1)$.

B. Stability Analysis for the Proposed Control Law

The range $r_{ij} = r_{ji} = \|\mathbf{p}_i - \mathbf{p}_j\|$ will be useful in analyzing the evolution of the multi-agent system but is not included in the implementation of the controller.

In addition to the formation stability results, we will show later that if $r_{ij} = r_{ji} > 0$ at some time t_0, for all i, j then it remains strictly positive for all $t \geq t_0$, i.e. we prove that collisions are avoided naturally by our formation control law and thus α_i is well-defined for all time.

Consider agent i with $v_i = \alpha_i^* - \alpha_i$ and heading β_i defined as before (6) and note that $\mathcal{N}_i = \{(i+1), (i-1)\}$. Obviously, agent i moves with a speed of $\alpha_i^* - \alpha_i$ and with a heading along the bisection of α_i. This (directly) affects how $\dot{\alpha}_{i\pm 1}$ evolves. If agents $i+1$ and $i-1$ are static, then

$$\begin{aligned} \dot{\alpha}_{i+1} &= -\frac{v_i}{r_{i(i+1)}} \sin(\frac{\alpha_i}{2}) \\ &= -\frac{1}{r_{i(i+1)}} \sin(\frac{\alpha_i}{2})(\alpha_i^* - \alpha_i) \end{aligned} \tag{7}$$

using the formula for the angular velocity in terms of the cross-radial component of the velocity of agent i. The sign is negative since if α_i increases, i.e. if $(\alpha_i^* - \alpha_i) > 0$, then α_{i+1} decreases. Similarly

$$\dot{\alpha}_{i-1} = -\frac{1}{r_{i(i-1)}} \sin(\frac{\alpha_i}{2})(\alpha_i^* - \alpha_i) \tag{8}$$

In addition, $\dot{\alpha}_i$ is affected directly by $\alpha_i^* - \alpha_i$. Note that $\sum_i \dot{\alpha}_i = 0$. Thus, when agents $i+1$ and $i-1$ are static we have

$$\begin{aligned} \dot{\alpha}_i &= \frac{(\alpha_i^* - \alpha_i)}{r_{i(i+1)}} \sin(\frac{\alpha_i}{2}) + \frac{(\alpha_i^* - \alpha_i)}{r_{i(i-1)}} \sin(\frac{\alpha_i}{2}) \\ &= \frac{r_{i(i+1)} + r_{i(i-1)}}{r_{i(i+1)} r_{i(i-1)}} \sin(\frac{\alpha_i}{2})(\alpha_i^* - \alpha_i) \\ &= \frac{\sin(\alpha_{i+1}) + \sin(\alpha_{i-1})}{r_{i(i+1)} \sin(\alpha_{i+1})} \sin(\frac{\alpha_i}{2})(\alpha_i^* - \alpha_i) \\ &= \frac{\sin(\alpha_{i+1}) + \sin(\alpha_{i-1})}{r_{i(i-1)} \sin(\alpha_{i-1})} \sin(\frac{\alpha_i}{2})(\alpha_i^* - \alpha_i) \end{aligned} \tag{9}$$

where the last three lines of (9) are equivalent via the sine rule. Now for future notational brevity let

$$f_{i(i+1)} = \frac{1}{r_{i(i+1)}} \sin(\frac{\alpha_{i+1}}{2}) \tag{10}$$

and let

$$g_i = \frac{r_{i(i+1)} + r_{i(i-1)}}{r_{i(i+1)} r_{i(i-1)}} \sin(\frac{\alpha_i}{2}) \tag{11}$$

where we note $g_i \geq 0$ and $f_{ij} \geq 0$ for all $i, j \in \{1, 2, 3\}$ when $\alpha_i \in [0, \pi]$, $\forall i$. Now, assuming all agents move with a motion governed by their individual control laws we have

$$\dot{\alpha}_i = g_i(\alpha_i^* - \alpha_i) - f_{i(i+1)}(\alpha_{i+1}^* - \alpha_{i+1}) - f_{i(i-1)}(\alpha_{i-1}^* - \alpha_{i-1}) \tag{12}$$

with $\alpha_i \in [0, \pi]$. The system of differential equations

$$\dot{\alpha} = \begin{bmatrix} -g_1 & f_{12} & f_{13} \\ f_{21} & -g_2 & f_{23} \\ f_{31} & f_{32} & -g_3 \end{bmatrix} \left(\alpha - \begin{bmatrix} \alpha_1^* \\ \alpha_2^* \\ \alpha_3^* \end{bmatrix} \right) \tag{13}$$

where

$$\alpha = \begin{bmatrix} \alpha_1 & \alpha_2 & \alpha_3 \end{bmatrix}^{\mathrm{T}} \tag{14}$$

is defined on a 2-simplex in α-space with vertices $\alpha = [\pi\ 0\ 0]^\top$, $\alpha = [0\ \pi\ 0]^\top$ and $\alpha = [0\ 0\ \pi]^\top$. We denote this manifold by $\mathcal{M}_\alpha$.

Define the control error $e_i = (\alpha_i - \alpha_i^*) \in [-\pi, \pi]$ for each agent i. Then the following differential system is obtained

$$\begin{aligned} \dot{e}_i = & -\frac{\sin(\alpha_{i+1}) + \sin(\alpha_{i-1})}{r_{i(i+1)} \sin(\alpha_{i+1})} \sin(\frac{\alpha_i}{2}) e_i + \\ & \frac{1}{r_{i(i+1)}} \sin(\frac{\alpha_{i+1}}{2}) e_{i+1} + \\ & \frac{1}{r_{i(i-1)}} \sin(\frac{\alpha_{i-1}}{2}) e_{i-1} \end{aligned} \tag{15}$$

Using both (10) and (11), then the system of differential equations (15) can be written succinctly as

$$\dot{e}_i = -g_i e_i + f_{i(i+1)} e_{i+1} + f_{i(i-1)} e_{i-1} \tag{16}$$

Note that $\dot{e}_i$ is a nonlinear differential equation since, for example, $\alpha_i = \alpha_i^* + e_i$ is dependent on the known constant α_i^* and also the error e_i. Stacking the system of differential equations (15) or (16) leads to

$$\dot{\mathbf{e}} = \mathbf{F}(\mathbf{e})\mathbf{e} \tag{17}$$

where

$$\mathbf{e} = \begin{bmatrix} e_1 & e_2 & e_3 \end{bmatrix}^{\mathrm{T}} \tag{18}$$

and where

$$\mathbf{F}(\mathbf{e}) = \begin{bmatrix} -g_1 & f_{12} & f_{13} \\ f_{21} & -g_2 & f_{23} \\ f_{31} & f_{32} & -g_3 \end{bmatrix} \tag{19}$$

where $\mathbf{e}$ is defined on a 2-simplex in $\mathbf{e}$-space with vertices $\mathbf{e} = [\pi - \alpha_1^*\ \ -\alpha_2^*\ \ -\alpha_3^*]^\top$, $\mathbf{e} = [-\alpha_1^*\ \pi - \alpha_2^*\ \ -\alpha_3^*]^\top$ and $\mathbf{e} = [-\alpha_1^*\ \ -\alpha_2^*\ \pi - \alpha_3^*]^\top$. We denote this manifold by $\mathcal{M}_e$. In fact, $\mathcal{M}_e$ is obtained directly from $\mathcal{M}_\alpha$ via a translation by $-[\alpha_1^*\ \alpha_2^*\ \alpha_3^*]^\top$. Again, $\mathbf{F}(\mathbf{e})$ is (significantly) nonlinear in $\mathbf{e}$ since $\alpha_i = \alpha_i^* + e_i$.

Figure 1 depicts the error manifold and shows six distinct error regions, $\mathfrak{R}_{i\pm}$, with $i \in \{1, 2, 3\}$. The index conventions will become clear subsequently.

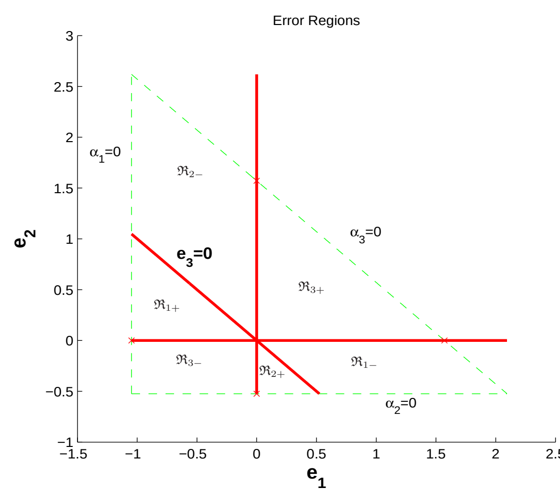

Fig. 1. A plot of the open error manifold showing six distinct regions and the boundaries of the manifold.

Note the regions are taken without boundary such that, for example, we can define $\mathfrak{R}_{3+}$ by

$$\mathbf{e} \in \mathfrak{R}_{3+} \iff \begin{bmatrix} 0 < e_1 < \pi - \alpha_1^* \\ 0 < e_2 < \pi - \alpha_2^* \\ -\alpha_3^* < e_3 < 0 \end{bmatrix} \tag{20}$$

For distinct $i, j, k \in \{1, 2, 3\}$, we chose the individual error regions to exhibit the following useful properties

$$\mathfrak{R}_{\mathrm{i}+} \ \Rightarrow\ \{e_j > 0, e_k > 0, e_i < 0, \dot{e}_i > 0\} \tag{21}$$

or

$$\mathfrak{R}_{\mathrm{i}-} \ \Rightarrow\ \{e_j < 0, e_k < 0, e_i > 0, \dot{e}_i < 0\} \tag{22}$$

where $e_i \in [-\alpha_i^*, \pi - \alpha_i^*] \subset [-\pi, \pi]$, $\forall i$ and $\sum_i e_i = 0$ must be enforced. The sign of the errors is taken directly from the definition of the region while the sign of a particular error velocity can be determined using the signs of the error and (17). *The inequalities are strict.* Note importantly that the simplex, or manifold $\mathcal{M}_e$ shifts in the error space depending on the desired configuration angles α_i^*. As such, error regions, $\mathfrak{R}_{\mathrm{i}\pm}$, can grow or shrink, and can disappear altogether. For example, take the case where $\alpha_1^* = \alpha_2^* = 0$ such that $\alpha_3^* = \pi$, then the only region in existence is $\mathfrak{R}_{3+}$.

Theorem 1. *The manifold $\mathcal{M}_e$ is a positively invariant set.*

Proof: To show that $\mathcal{M}_e$ is positively invariant we show that for any $e_i \in \mathcal{M}_e$, then it is impossible for e_i to escape $\mathcal{M}_e$. Note that $e_i \in [-\alpha_i^*, \pi - \alpha_i^*] \subset [-\pi, \pi]$. Thus, let us consider the right-sided limit,

$$\begin{aligned}
\lim_{e_i \to -\alpha_i^{*+}} \dot{e}_i &= \frac{1}{r_{i(i+1)}} \sin\left(\frac{\alpha_{(i+1)}}{2}\right) e_{i+1} + \\
&\quad \frac{1}{r_{i(i-1)}} \sin\left(\frac{\alpha_{(i-1)}}{2}\right) e_{i-1} \\
&= \frac{e_{i+1}}{r_{i(i+1)}} \quad \text{if} \quad \begin{array}{l} e_{i+1} \to (\pi - \alpha_{i+1}^*)^- \\ e_{i-1} \to -\alpha_{i-1}^{*\,+} \end{array} \\
&= \frac{e_{i-1}}{r_{i(i-1)}} \quad \text{if} \quad \begin{array}{l} e_{i+1} \to -\alpha_{i+1}^{*\,+} \\ e_{i-1} \to (\pi - \alpha_{i-1}^*)^- \end{array} \\
&> 0
\end{aligned} \tag{23}$$

which implies e_i cannot escape $\mathcal{M}_e$ in one direction. A similar computation shows that e_i cannot escape $\mathcal{M}_e$ in the other direction, i.e. by following $e_i \to \pi - \alpha_i^*$ through the boundary of the manifold. That is

$$\begin{aligned}
\lim_{e_i \to (\pi - \alpha_i^*)^-} \dot{e}_i &= -\frac{r_{i(i+1)} + r_{i(i-1)}}{r_{i(i+1)} r_{i(i-1)}} e_i \\
&< 0
\end{aligned} \tag{24}$$

which completes the proof. □ ■

Note that technically, once inside $\mathcal{M}_e$, there are only three possible escape routes. In the proof of Theorem 1 we show that none of these routes can be taken. Given that $\mathcal{M}_e$ is a positively invariant set, we state the following result which ensures the formation is well-defined for all time t, i.e. the angles α_i are well defined for all time.

Theorem 2. *Suppose that $\mathbf{p}_i(t_0) \neq \mathbf{p}_j(t_0)$ for $i \neq j$ at some time t_0. Then, $\mathbf{p}_i(t) \neq \mathbf{p}_j(t)$ for $i \neq j$ for all $t \geq t_0$, i.e. for all $t \geq t_0$ we have $\|\mathbf{p}_i(t) - \mathbf{p}_j(t)\| > 0$.*

Proof: In order for $\mathbf{p}_i(t) = \mathbf{p}_j(t)$ at some time $t > t_0$ there must exist a time interval $[t-\epsilon, t]$ with $t - \epsilon \geq t_0$ on which $\beta_i = \phi_{ij}$ and/or $\beta_j = \phi_{ji}$ for any $\epsilon \geq dt$. We now show that no such time interval can exist. We consider now, with no loss of generality, that $\beta_i = \phi_{ij}$. Note that $\beta_i = \phi_{ij}$ on $[t-\epsilon, t]$ then implies $\alpha_i = 0$ which implies $\alpha_j = 0$ or $\alpha_j = \pi$ on the entire interval $[t-\epsilon, t]$. If $\alpha_j(t-\epsilon) = \pi$ then at time $t-\epsilon+dt$ we immediately have $\beta_i \neq \phi_{ij}$ since $\alpha_j(t-\epsilon+dt) < \pi$. To see this note that $\alpha_j(t-\epsilon) = \pi$ implies

$$\dot{\alpha}_j = -g_j(\alpha_j - \alpha_j^*) \quad \text{on} \quad [t-\epsilon, t-\epsilon+dt] \tag{25}$$

which is strictly negative unless $\alpha_j^* = \pi$ which according to Assumption 1 would imply that both agents $i, k \neq j$ are also at equilibrium. Similarly, if $\alpha_j = 0$ then at time $t - \epsilon + dt$ we immediately have $\beta_i \neq \phi_{ij}$ since $\alpha_j(t - \epsilon + dt) > 0$. □ ■

The previous result ensures collisions are avoided naturally by the formation. The following result characterizes the equilibrium points of the system.

Theorem 3. *The system (17) is at equilibrium $\dot{\mathbf{e}} = 0$ if and only if $\mathbf{e} = 0$.*

Proof: The sufficiency of $\mathbf{e} = 0$ is obvious. To prove necessity, suppose firstly that the state of the system is in one of the six distinct regions $\mathfrak{R}_{\mathrm{i}+}$ or $\mathfrak{R}_{\mathrm{i}-}$ defined using (21) or (22). Using (21) or (22) it is clear $\dot{e}_i \neq 0$ for at least one i, i.e. the system is not at equilibrium.

Now it remains to show that on the manifold $\mathcal{M}_e$ there are no equilibrium points on the boundaries in between the error regions. Denote such a boundary via

$$\Sigma_{\mathrm{i+j-}} = \{\partial\mathfrak{R}_{\mathrm{i}+} \cap \partial\mathfrak{R}_{\mathrm{j}-}\}/\{\mathbf{0}\} = \Sigma_{\mathrm{j-i+}} \tag{26}$$

and note we consider only boundaries with strictly positive length, i.e. a strictly positive 1-d Hausdorff measure. Now following our derivation of the error regions $\mathfrak{R}_{\mathrm{i}+}$ we find that

$$\mathbf{e} \in \Sigma_{\mathrm{i+j-}} \iff \begin{bmatrix} -\alpha_i^* < e_i < 0 \\ 0 < e_j < \pi - \alpha_j^* \\ e_k = 0 \end{bmatrix} \tag{27}$$

which implies, using (16), that $\dot{e}_i > 0$ and $\dot{e}_j < 0$ and thus $\dot{\mathbf{e}} \neq 0$. This completes the proof. □ ■

We introduce the following theorem which will form the basis of our subsequent stability proof.

Theorem 4 (Poincare-Bendixson [34])**.** *Let $\mathcal{M} \subset \mathbb{R}^2$ be a compact, positively invariant two-manifold containing a finite number of fixed points. Let $\mathbf{x} \in \mathcal{M}$ and consider the ω-limit set $\omega(\mathbf{x})$. Then one of the following possibilities holds:*

1) *$\omega(\mathbf{x})$ is an equilibrium point;*
2) *$\omega(\mathbf{x})$ is a closed orbit;*
3) *$\omega(\mathbf{x})$ consists of a finite number of fixed points $\overline{\mathbf{x}}_1$, ..., $\overline{\mathbf{x}}_m$ and orbits γ with $\alpha(\gamma) = \overline{\mathbf{x}}_i$ and $\omega(\gamma) = \overline{\mathbf{x}}_j$,*

where $\alpha(\gamma)$ means the α-limit set of every point γ.

The intuition behind the Poincare-Bendixson theorem is that all bounded trajectories in a planar region (or two-manifold) must converge to an equilibrium point, a limit cycle, or a union of fixed points and the trajectories connecting them, i.e. so-called homoclinic or heteroclinic orbits.

We know there is only a single equilibrium and that $\mathcal{M}_e$ is positively invariant. We now show there are no closed orbits.

Theorem 5. *The system (17) has no closed orbits in $\mathcal{M}_e$.*

Proof: Consider the arc between adjacent regions given by

$$\Sigma_{\mathrm{i+j-}} = \{\partial\mathfrak{R}_{\mathrm{i}+} \cap \partial\mathfrak{R}_{\mathrm{j}-}\}/\{\mathbf{0}\} = \Sigma_{\mathrm{j-i+}} \tag{28}$$

with strictly positive length, i.e. a strictly positive 1-d Hausdorff measure. There are six such ‘well-defined’ sets $\Sigma_{\mathrm{i+j-}} =$

$\Sigma_{\mathrm{j-i+}}$. Now define

$$\Sigma = \Sigma_{3+1-} \cup \Sigma_{1-2+} \cup \Sigma_{2+3-} \cup \Sigma_{3-1+} \cup \Sigma_{1+2-} \cup \Sigma_{2-3+} \tag{29}$$

and note for clarity that $\Sigma \cap \{\mathbf{0}\} = \emptyset$. Note that any closed orbit must enclose the origin [34] and thus intersect every well-defined boundary $\Sigma_{\mathrm{i+j-}}$. As a consequence, if the origin is on a vertex of the manifold $\mathcal{M}_e$, i.e. if the desired configuration is a line formation, then obviously no closed orbits exist. Otherwise, the strategy is to show that any positive orbit $\psi^+(\mathbf{e})$ of (17) intersects Σ in a strictly monotone sequence approaching the origin (if it intersects it in more than a point). That is, we show that if $\mathbf{e}_{m+1}$ is the $(m+1)^{\mathrm{th}}$ intersection of Σ then $\|\mathbf{e}_{m+1}\| < \|\mathbf{e}_m\|$. Note that

$$\begin{aligned} \mathbf{e} \in \Sigma_{\mathrm{i+j-}} \quad &\Rightarrow \quad \dot{e}_i > 0,\ e_i < 0 \ \text{ and } \ \dot{e}_j < 0,\ e_j > 0 \\ &\Rightarrow \quad e_k = 0 \ \text{ and } \ \|\mathbf{e}\| = |e_j| \end{aligned} \tag{30}$$

using the definition of regions where $i, j, k \in \{1, 2, 3\}$ are distinct indices. We proceed using an inductive-like argument. Suppose that $\mathbf{e}_m$ is the m^{th} intersection of Σ (which also intersects $\Sigma_{\mathrm{i+j-}}$) for the positive orbit $\psi_t^+(\mathbf{e}_m)$ starting at $t = t_m$. Define a time t_{m+1} and mark $\mathbf{e}_{m+1}$ as the $(m+1)^{\mathrm{th}}$ intersection of Σ with $\mathbf{e}_{m+1} = \psi^+_{t_{m+1}}(\mathbf{e}_m)$. There exists a time $t_{m^+} \in (t_m, t_{m+1}]$ at which $\psi^+_{t_{m^+}}(\mathbf{e}_m)$ is in (i) $\Sigma_{\mathrm{i+j-}}$ or (ii) $\mathfrak{R}_{i+}$ or (iii) $\mathfrak{R}_{j-}$. We ignore the trivial case $\psi^+_{t_{m^+}}(\mathbf{e}_m) \in \{\mathbf{0}\}$ for some $t_{m^+} \in (t_m, t_{m+1})$.

(Case i): If $\psi^+_{t_{m^+}}(\mathbf{e}_m)$ is in $\Sigma_{\mathrm{i+j-}}$ then $t_{m^+} = t_{m+1}$ and $0 < e_j(t_{m+1}) < e_j(t_m)$ using (30). It follows that $\|\mathbf{e}_{m+1}\| < \|\mathbf{e}_m\|$. We restart the argument at time $t = t_{m+1}$.

(Case ii): If $\psi^+_{t_{m^+}}(\mathbf{e}_m)$ is in $\mathfrak{R}_{i+}$ then $e_j > 0$, $e_k > 0$ and $\dot{e}_i = -\dot{e}_j - \dot{e}_k > 0$ which implies $-\dot{e}_j > \dot{e}_k$. The relevant boundaries of $\mathfrak{R}_{i+}$ are $\Sigma_{\mathrm{i+j-}}$ and $\Sigma_{\mathrm{i+k-}}$ for distinct $i, j, k \in \{1, 2, 3\}$. Now if $\mathbf{e}_{m+1} \in \Sigma_{\mathrm{i+j-}}$ then

$$\int_{t_m}^{t_{m+1}} \dot{e}_k(\tau) d\tau = 0 \quad \Rightarrow \quad \int_{t_m}^{t_{m+1}} \dot{e}_j(\tau) d\tau < 0 \tag{31}$$

which immediately implies $|e_j(t_{m+1})| < |e_j(t_m)|$. Using (30) it follows that $\|\mathbf{e}_{m+1}\| < \|\mathbf{e}_m\|$ and we can then restart the argument at time $t = t_{m+1}$. Now if instead $\mathbf{e}_{m+1} \in \Sigma_{\mathrm{i+k-}}$ then $-\dot{e}_j > \dot{e}_k$ implies

$$\int_{t_m}^{t_{m+1}} \dot{e}_j(\tau) d\tau = -e_j(t_m) \ \Rightarrow \ \int_{t_m}^{t_{m+1}} \dot{e}_k(\tau) d\tau < e_j(t_m) \tag{32}$$

and since $e_k(t_m) = 0$ we have $|e_k(t_{m+1})| < |e_j(t_m)|$. The consequence of this last fact is that $\|\mathbf{e}_{m+1}\| < \|\mathbf{e}_m\|$ and we can then restart the argument at time $t = t_{m+1}$.

(Case iii): If $\psi^+_{t_{m^+}}(\mathbf{e}_m)$ is in $\mathfrak{R}_{j-}$ then the argument follows similarly to that given in case (ii). □ ■

Note that Theorem 5 could be interpreted as a proof of asymptotic convergence of any solution of (17) to the origin. The following result makes this convergence precise.

Theorem 6 (The Main Result)**.** *The equilibrium* $\mathbf{e} = 0$ *of the error system (17) is globally asymptotically stable.*

Proof: We use the Poincare-Bendixson theorem. Consider $\mathcal{M}_e^- = \mathrm{cl}(\mathcal{M}_e)$ where $\mathrm{cl}(\cdot)$ denotes set closure. Note that $\mathcal{M}_e^-$ is now compact with a single equilibrium and no closed orbits, via Theorems 3 and 5. Clearly, $\mathbf{e}(0)$ must be in $\mathcal{M}_e \subset \mathcal{M}_e^-$ and $\mathcal{M}_e$ acts as a positively invariant set, via Theorem 1. The Poincare-Bendixson theorem then states the ω-set of any initial error in $\mathcal{M}_e^-$ contains only $\mathbf{e} = 0$. Global asymptotic stability is assured. □ ■

The previous result is our main result and concerns the global asymptotic formation stability for all desired configurations. Using a linearization argument, we can comment on the convergence rate for almost all desired formations.

Theorem 7. *If* $\alpha_i^* \in (0, \pi)$ *then solutions of (17) with any initial condition in* $\mathcal{M}_e$ *will converge asymptotically to the origin and there exists a neighbourhood* $\mathcal{U}$ *of the origin within which solutions converge at an exponential rate.*

Proof: The asymptotic stability of the origin for all desired configurations, i.e. $\alpha_i^* \in [0, \pi]$, and all initial positions follows from the main result, Theorem 6. Now note that $e_k = -e_i - e_j$ for distinct $i, j, k \in \{1, 2, 3\}$. We then reduce the dimension of (17) and obtain

$$\begin{aligned} \dot{\mathbf{e}}_{ij} \quad &= \quad \mathbf{F}_{ij}(\mathbf{e})\mathbf{e}_{ij} \\ \left[\begin{array}{c} e_i \\ e_j \end{array} \right]^{\cdot} \quad &= \quad \left[\begin{array}{cc} -(g_i + f_{ik}) & (f_{ij} - f_{ik}) \\ (f_{ji} - f_{jk}) & -(g_j + f_{jk}) \end{array} \right] \left[\begin{array}{c} e_i \\ e_j \end{array} \right] \end{aligned} \tag{33}$$

with $g_i > 0$ and $f_{ij} > 0$ when $\alpha_i \in (0, \pi)$ and $g_i = f_{ji} + f_{ki}$. Linearization of (33) about the point $\mathbf{e} = 0$ leads to

$$\dot{\mathbf{e}} = \mathbf{A}_{ij}(\alpha^*)\mathbf{e} \tag{34}$$

where $\mathbf{A}_{ij}(\alpha^*)$ is a constant matrix and denotes the gradient of $\mathbf{F}_{ij}(\mathbf{e})\mathbf{e}_{ij}$ with respect to $\mathbf{e}$ and evaluated at $\mathbf{e} = 0$. Note that $\mathbf{A}_{ij}(\alpha^*) = \mathbf{F}_{ij}(\mathbf{e})|_{\alpha_i = \alpha_i^*}$. It is then easy to verify that

$$\mathrm{tr}(\mathbf{A}_{ij}(\alpha^*)) < 0 \tag{35}$$

$$\det(\mathbf{A}_{ij}(\alpha^*)) > 0 \tag{36}$$

for all $\alpha_i^* \in (0, \pi)$. Now it follows that $\mathbf{A}_{ij}(\alpha^*)$ is stable, i.e. $\mathbf{A}_{ij}(\alpha^*)$ has negative real eigenvalues, for all $\alpha_i^* \in (0, \pi)$. Now within a neighborhood of the origin $\mathcal{U}$ it follows from the Hartman-Grobman theorem [34] that solutions of (17) converge at an exponential rate when $\alpha_i^* \in (0, \pi)$.

When the desired formation is a line then linearization is inconclusive with one negative real eigenvalue and one zero eigenvalue (and additional tests would be required). □ ■

We conjecture that if the desired formation is a line then $\mathbf{e} = 0$ is also locally exponentially stable (we know it is globally asymptotically stable from Theorem 6). However, we do not explore this particular case further.

The neighborhood $\mathcal{U}$ can be made large by considering certain Lyapunov functions explicitly but the value in doing so is limited given the existence of Theorem 6. In addition, as discussed in the next subsection, we could not find a suitable Lyapunov function to show global stability. Also, the simulation results indicate an exponential convergence rate for the entire formation trajectory.

Finally, we make the following useful remark.

Remark 1. *Denote a formation of agents at equilibrium, i.e. with* $\alpha_i = \alpha_i^*$*, as an equilibrium formation which is defined by* *the agent positions $\mathbf{p}_i^*$ at equilibrium. An equilibrium formation is invariant to scale, rotation and translation of the formation as a whole or reflection of any agent i about the triangle edge formed by agents $i+1$ and $i-1$.*

This last remark is given for completeness and illustrates the simple fact that transforming an *equilibrium formation* in any of the referred to ways does not change the equilibrium status of the formation. However, it is of course still true that given $\mathbf{p}_i(0)$ for all i, the desired formation $\mathbf{p}_i^*$ is unique (given the standard uniqueness theorem [34]).

C. Discussion on the Method of Proof

Note that we could not find a suitable Lyapunov function that would prove global stability for all desired formations given any initial configuration. In particular, testing the negative-definiteness of the time-derivative for various candidates was a significant hurdle. Variations on a number of quadratic-type candidate functions failed the negative-definite test in simulation. Indeed, $\mathbf{F}_{ij}$ in (33) is not negative definite for $\alpha_i \in [0, \pi]$. However, it was clear to us that the system evolved on a positively-invariant set and that there was only a single equilibrium. Moreover, we suspected that no limit cycles were present. As such, given the dimension of the system manifold, we know the Poincare-Bendixson theorem provides a rigorous statement concerning the asymptotic behaviour of the system trajectories. Thus, we chose to seek a globally asymptotic convergence proof through the Poincare-Bendixson theorem. An alternative route we considered was via linearization (which does lead to local exponential stability for almost all desired configurations). The disadvantage of using only linearization is that global stability does not follow (and even local exponential stability does not follow for desired line configurations using linearization alone). In any case, we believe the analysis given in this paper provides a deep insight into the nature of the proposed vector field on the manifold of interest.

III. Examples

In this section we demonstrate the algorithm developed in this paper for distributed formation control with bearing-only measurements and relative angular constraints.

1) Triangle to Triangle Formation: The first example illustrates how the formation converges to an arbitrarily specified triangle (so long as the triangle is feasible) given a random initial triangle configuration. The desired triangle formation in this case is characterized by $\alpha_1^* = \pi/6$, $\alpha_2^* = \pi/4$ and $\alpha_3^* = 7\pi/12$. The formation motion is illustrated in Figure 2 along with the convergence of $|e_i|$ to zero.

The initial position of the three agents are randomly distributed in $\mathcal{M}_\alpha$ and the figure illustrates the trajectories of each agent as the formation converges upon the desired shape. This example illustrates that the control law can generate arbitrary triangle formations.

2) Line to Triangle Formation: Consider now the case involving three agents initially collinear. The desired formation is a triangle characterized by $\alpha_1^* = \pi/3$, $\alpha_2^* = \pi/6$ and

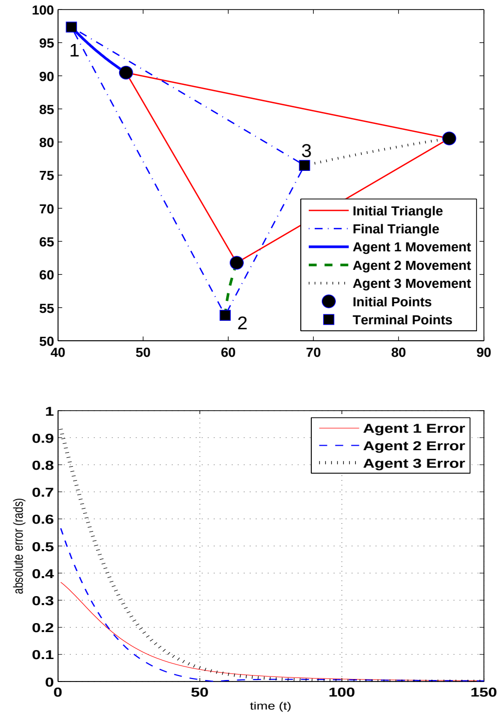

Fig. 2. The motion of the formation with a desired terminal constraint of $\alpha_1^* = \pi/6$, $\alpha_2^* = \pi/4$ and $\alpha_3^* = 7\pi/12$.

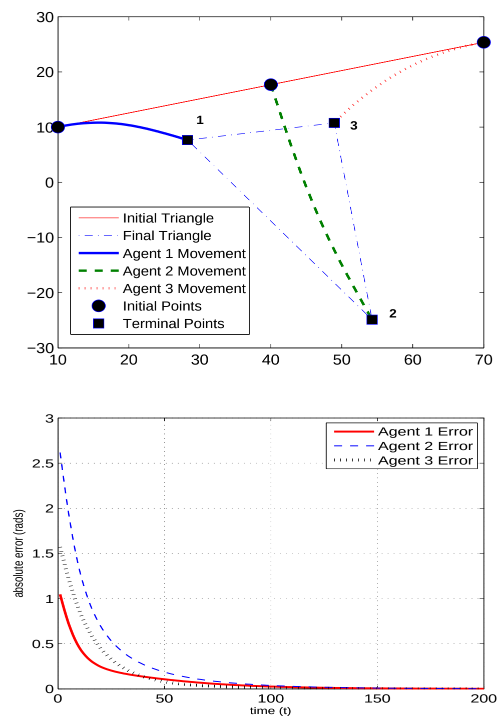

Fig. 3. The motion of a triangular formation consisting of three mobile agents initially in a collinear position with desired terminal constraints $\alpha_1^* = \pi/3$, $\alpha_2^* = \pi/6$ and $\alpha_3^* = \pi/2$.

$\alpha_3^* = \pi/2$. The formation motion is illustrated in Figure 3 along with the control error for each agent.

The convergence of the three agents is illustrated in Figure 3 along with the convergence of $|e_i|$ to zero for all $i \in \{1, 2, 3\}$. This example illustrates that the control law is not affected by initial agent collinearity.

3) Triangle to Line Formation: This example shows the convergence of an initially random triangle formation to a desired line formation. The desired formation is characterized by $\alpha_1^* = \alpha_2^* = 0$ and $\alpha_3^* = \pi$.

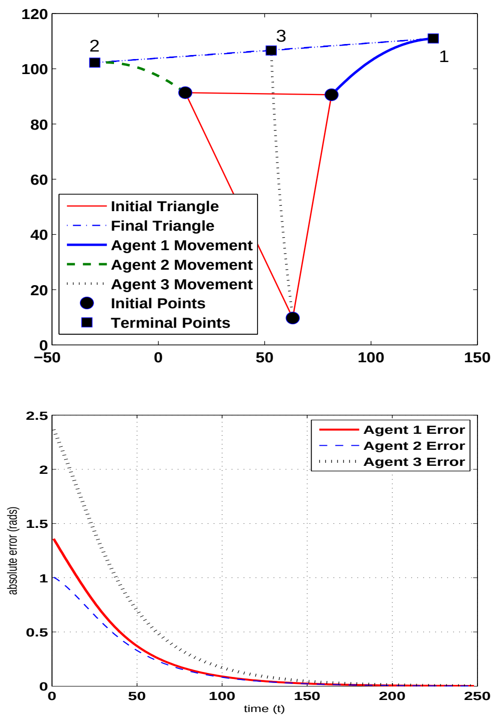

Fig. 4. The motion of a triangular formation consisting of three mobile agents starting in a random triangle and given a desired collinearity condition.

The convergence of the three agents is illustrated in Figure 4 along with the convergence of $|e_i|$ to zero for all $i \in \{1, 2, 3\}$. This example illustrates that we can steer an arbitrary initial triangle formation to a collinear formation.

4) Line to Line Formation: Finally, we consider the case of changing from an initial line formation with $\alpha_1 = 0$, $\alpha_2 = \pi$ and $\alpha_3 = 0$ to another (desired) line formation with $\alpha_1^* = 0$, $\alpha_2^* = 0$ and $\alpha_3^* = \pi$. The order of the agents along the line changes from the initial formation to the desired formation. The formation motion is illustrated in Figure 5 along with the control error for each agent.

The convergence of the three agents is illustrated in Figure 5 along with the convergence of $|e_i|$ to zero for all $i \in \{1, 2, 3\}$. Note that agents 2 and 3 do not collide but do indeed swap places in the formation configuration.

5) A Phase Portrait for the System: For illustrative purposes, we plot the phase portrait of the reduced system (33) when the desired formation is an equilateral triangle, i.e. when $\alpha_1^* = \alpha_2^* = \alpha_3^* = \pi/3$.

In Figure 6 we see the manifold $\mathcal{M}_e$ and the behaviour of the vector field on this manifold for a particular desired formation.

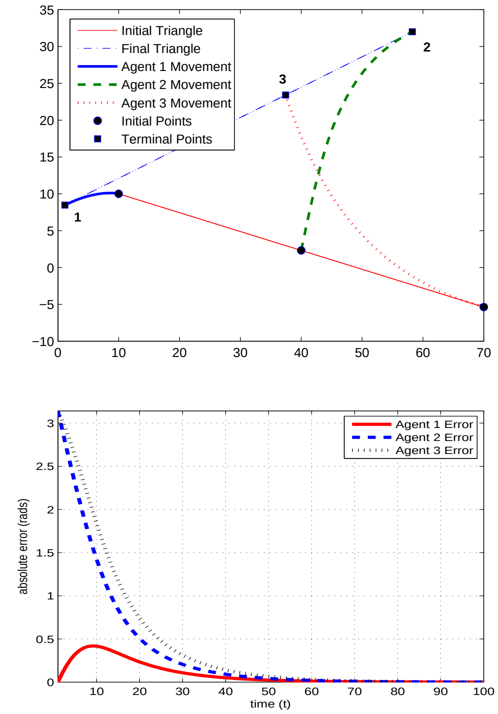

Fig. 5. The motion of a triangular formation consisting of three mobile agents initially in a collinear position with a desired condition specified by another collinear formation with a different agent ordering.

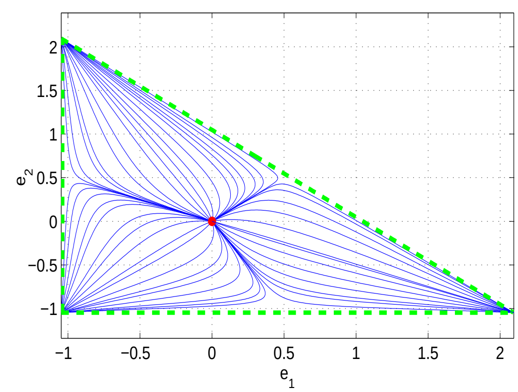

Fig. 6. Phase portrait of the reduced error system (33) when the desired formation is an equilateral triangle.

IV. Discussion

The case where $\alpha_i^* = 0$, $\alpha_j^* \neq 0$ and $\alpha_k^* = \pi - \alpha_j^*$ is a special case where, in the desired configuration, agent i must be placed infinitely far from the other two agents. Applying the derived control law in this case leads to agent j and agent k becoming coincident in the limit as $t \to \infty$. We note that our control law is applicable when $\alpha_i^* = \epsilon$, $\alpha_j^* \neq 0$ and $\alpha_k^* = \pi - \alpha_j^* - \epsilon$ for an arbitrarily small $\epsilon > 0$ and that inter-agent collisions are naturally avoided in such cases. In practice this is generally sufficient. We also believe an extension to the control law to account for such cases is also possible but the benefits of doing so are rather superficial.

An extension to the problem of formation control with an arbitrary number of sensors is the next step and requires one to specify the form of the agent interaction graph which in turn specifies the constraint network for the formation. In addition, proving global stability is likely to be non-trivial as the Poincare-Bendixson theorem employed in this paper is limited to scenarios involving only three agents.

V. Conclusion

This paper introduced a solution to the distributed bearing-only triangular formation control problem with angle-only inter-agent constraints. While the distance-based formation control problem has been extensively considered in the literature, the problem of bearing-only formation control is less studied. The solution provided in this paper requires only that each agent measure the bearing to the remaining two agents in a local coordinate system. Then, if each agent is given a desired interior angle subtended at itself by the other two agents, and assuming the set of desired interior angles is feasible, then the group of agents is shown to converge to the desired formation from any initial position.

VI. Acknowledgement

The authors would like to thank the reviewers and editors for their insightful comments which have significantly improved the presentation of our work.

References

[1] A.N. Bishop, B. Fidan, B.D.O. Anderson, K. Dogancay, and P.N. Pathirana. Optimality analysis of sensor-target geometries in passive localization: Part 1 - Bearing-only localization. In *Proc. of the 3rd International Conference on Intelligent Sensors, Sensor Networks, and Information Processing*, Melbourne, Australia, December 2007.

[2] A.N. Bishop, B. Fidan, B.D.O. Anderson, P.N. Pathirana, and K. Dogancay. Optimality analysis of sensor-target geometries in passive localization: Part 2 - Time-of-arrival based localization. In *Proc. of the 3rd International Conference on Intelligent Sensors, Sensor Networks, and Information Processing*, Melbourne, Australia, December 2007.

[3] A. Jadbabaie, J. Lin, and A.S. Morse. Coordination of groups of mobile autonomous agents using nearest neighbor rules. *IEEE Transactions on Automatic Control*, 48(6):9881001, June 2003.

[4] A.V. Savkin. Coordinated collective motion of groups of autonomous mobile robots: Analysis of vicsek's model. *IEEE Transactions on Automatic Control*, 49(6):981–983, June 2004.

[5] J.A. Fax and R.M. Murray. Information flow and cooperative control of vehicle formations. *IEEE Transactions on Automatic Control*, 49(9):1464–1476, September 2004.

[6] L. Moreau. Stability of multiagent systems with time-dependent communication links. *IEEE Transactions on Automatic Control*, 50(2):169–182, February 2005.

[7] R. Olfati-Saber. Flocking for multi-agent dynamic systems: Algorithms and theory. *IEEE Transactions on Automatic Control*, 51(3):401–420, March 2006.

[8] N. Moshtagh and A. Jadbabaie. Distributed geodesic control laws for flocking of nonoholonomic agents. *IEEE Transactions on Automatic Control*, 52(4):681–686, April 2007.

[9] V. Gazi. Stability analysis of swarms. *IEEE Transactions on Automatic Control*, 48(4):692–697, April 2003.

[10] E. Rimon and D.E. Koditschek. Exact robot navigation using artificial potential functions. *IEEE Transactions on Robotics and Automation*, 8(5):501–518, October 1992.

[11] R. O. Saber and R. M. Murray. Distributed cooperative control of multiple vehicle formations using structural potential functions. In *Proceedings of the 15th IFAC World Congress*, pages 1–7, Barcelona, Spain, July 2002.

[12] C. Belta and V. Kumar. Abstractions and control policies for a swarm of robots. *IEEE Transactions on Robotics*, 20(5):865–875, May 2004.

[13] Z. Lin, M.E. Broucke, and B.A. Francis. Local control strategies for groups of mobile autonomous agents. *IEEE Transactions on Automatic Control*, 49(4):622–629, April 2004.

[14] V. Gazi. Swarm aggregations using artificial potentials and sliding-mode control. *IEEE Transactions on Robotics*, 21(6):1208–1214, December 2005.

[15] V. Kumar, N.E. Leonard, and A.S. Morse (Editors). *Cooperative Control*, volume 309 of *Lecture Notes in Control and Information Sciences*. Springer-Verlag, New York, NY, 2004.

[16] W. Ren and R.W. Beard. A decentralized scheme for spacecraft formation flying via the virtual structure approach. *AIAA Journal of Guidance, Control and Dynamics*, 27(1):73–82, 2004.

[17] P. Ogren, E. Fiorelli, and N.E. Leonard. Cooperative control of mobile sensor networks: Adaptive gradient climbing in a distributed environment. *IEEE Transactions on Automatic Control*, 49(8):1292–1302, August 2004.

[18] J. Cortes, S. Martinez, T. Karatas, and F. Bullo. Coverage control for mobile sensing networks. *IEEE Transactions on Robotics*, 20(2):243255, February 2004.

[19] E. Fiorelli, N.E. Leonard, P. Bhatta, D.A. Paley, R. Bachmayer, and D.M. Fratantoni. Multi-AUV control and adaptive sampling in Monterey Bay. *IEEE Transactions on Oceanic Engineering*, 31(4):935–948, October 2006.

[20] N.E. Leonard, D.A. Paley, Lekien F., R. Sepulchre, Fratantoni D.M., and R.E. Davis. Collective motion, sensor networks and ocean sampling. *Proceedings of the IEEE*, 95(1):48–74, January 2007.

[21] R. O. Saber and R. M. Murray. Graph rigidity and distributed formation stabilization of multi-vehicle systems. In *Proceedings of the 41st IEEE Conference on Decision and Control*, pages 2965–2971, Las Vegas, Nevade, USA, 2002.

[22] J. Baillieul and A. Suri. Information patterns and hedging Brockett's theorem controlling vehicle formations. In *Proceedings of the 42nd IEEE Conference on Decision and Control*, pages 556–563, Maui, Hawaii, USA, December 2003.

[23] Z. Lin, B.A. Francis, and M. Maggiore. Necessary and sufficient graphical conditions for formation control of unicycles. *IEEE Transactions on Automatic Control*, 50(1):121–127, January 2005.

[24] B.D.O Anderson, C. Yu, S. Dasgupta, and A.S. Morse. Control of a three-coleader formation in the plane. *Systems and Control Letters*, 56:573–578, 2007.

[25] T. Eren, D.K. Goldenberg, W. Whiteley, Y.R. Yang, A.S. Morse, B.D.O. Anderson, and P.N. Belhumeur. Rigidity, computation, and randomization in network localization. In *Proceedings of the International Joint Conference of the IEEE Computer and Communications Societies*, pages 2673–2684, Hong Kong, March 2004.

[26] J.M. Hendrickx, B.D.O. Anderson, J-C. Delvenne, and V.D. Blondel. Directed graphs for the analysis of rigidity and persistence in autonomous agents systems. *International Journal of Robust and Nonlinear Control*, 17(10-11):960–981, 2006.

[27] C. Yu, J.M. Hendrickx, B. Fidan, B.D.O Anderson, and V.D. Blondel. Three and higher dimensional autonomous formations: Rigidity, persistence and structural persistence. *Automatica*, 43(3):387–402, 2007.

[28] T. Eren, W. Whiteley, and P. N. Belhumeur. Using angle of arrival (bearing) information in network localizationn. In *Proceedings of the 45th IEEE Conference on Decision and Control*, San Diego, California, USA, December 2006.

[29] A.G. Lindgren and K.F. Gong. Position and velocity estimation via bearing observations. *IEEE Transactions on Aerospace and Electronic Systems*, 14(4):564–577, July 1978.

[30] S.C. Nardone, A.G. Lindgren, and K.F. Gong. Fundamental properties and performance of conventional bearings-only target motion analysis. *IEEE Transactions on Automatic Control*, 29(9):775–787, 1984.

[31] M. Gavish and A.J. Weiss. Performance analysis of bearing-only target location algorithms. *IEEE Transactions on Aerospace and Electronic Systems*, 28(3):817–827, 1992.

[32] S.G. Loizou and V. Kumar. Biologically inspired bearing-only navigation and tracking. In *Proceedings of the 46th IEEE Conference on Decision and Control*, pages 1386–1391, New Orleans, LA, December 2007.

[33] N. Moshtagh, N. Michael, A. Jadbabaie, and K. Daniilidis. Vision-based, distributed control for motion coordination of nonholonomic robots. *IEEE Transactions on Robotics*, 25(4):851–860, August 2009.

[34] S. Wiggins. *Introduction to Applied Nonlinear Dynamical Systems and Chaos*. Springer-Verlag, New York, NY, 1990.